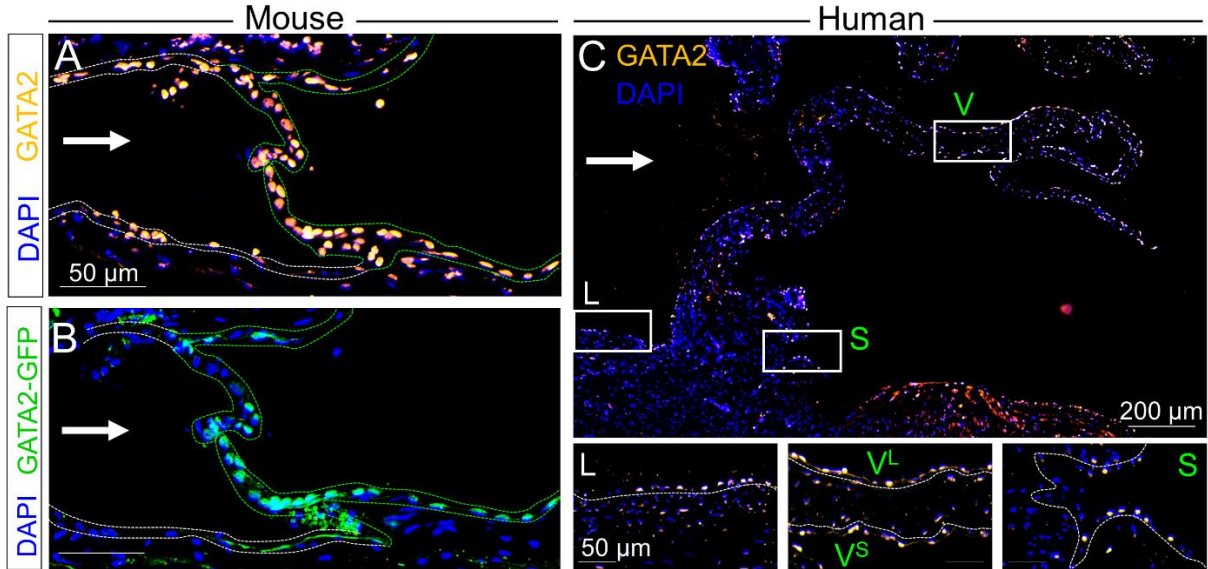
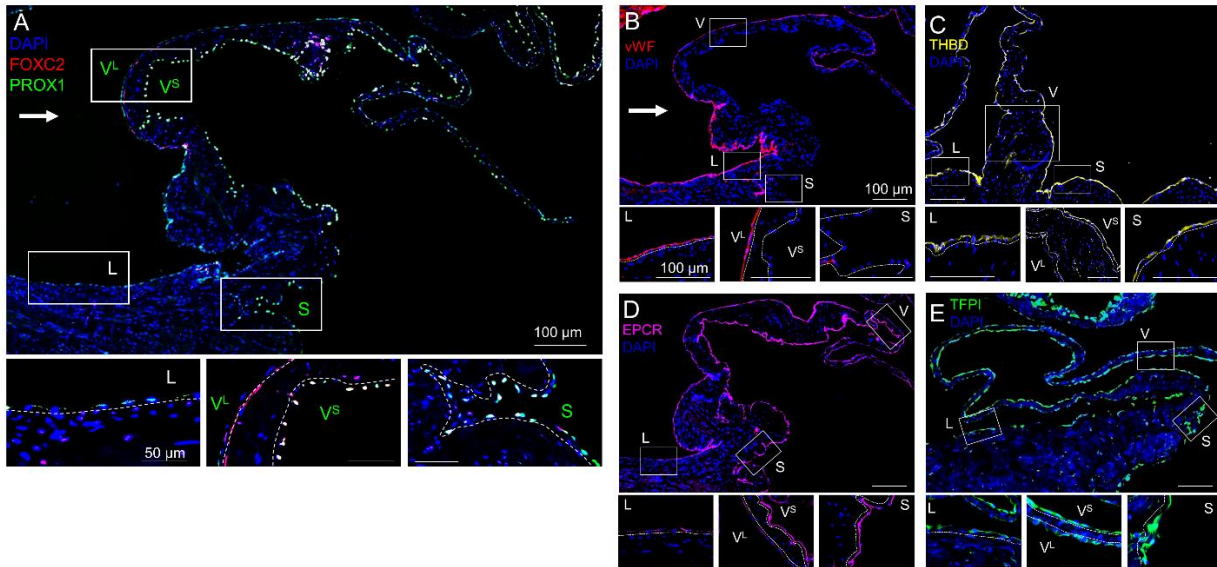


Supplemental Figure 1.



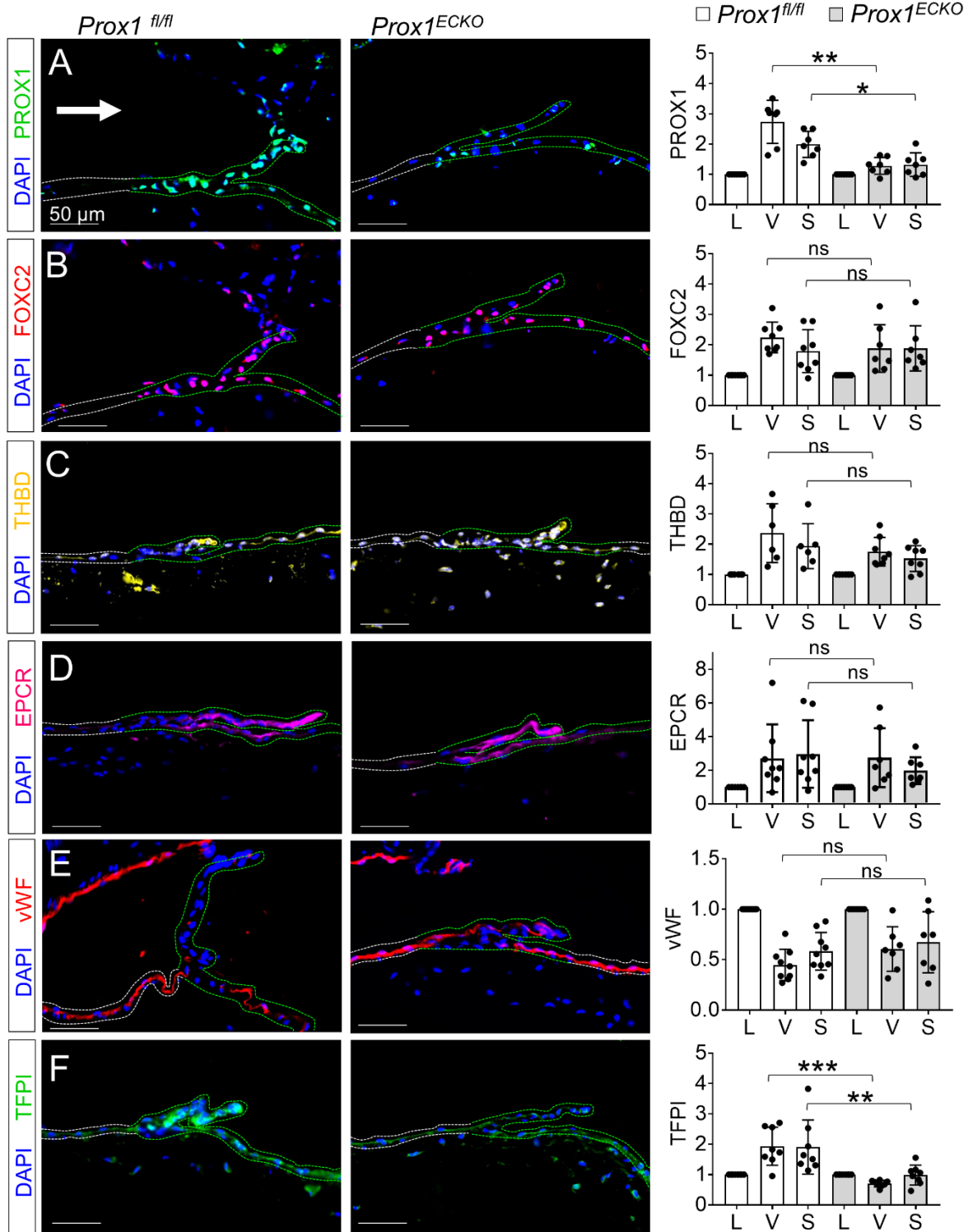
Supplemental Figure 1. GATA2 expression in mouse and human venous peri-valvular endothelial cells. **A**, Immunostaining for GATA2 revealed similar levels in the nuclei of endothelial cells lining the vessel lumen (L), valve (V), and valve sinus (S) of the mouse saphenous vein. **B**, Immunostaining for GFP in GATA2-GFP transgenic mice in which GFP is driven by a 3.1 kilobase length of GATA2 5' genomic DNA revealed elevated levels in the nuclei of endothelial cells lining the valve (V), and valve sinus (S) compared with those lining the vessel lumen (L) of the mouse saphenous vein. **C**, Immunostaining for GATA2 revealed similar levels in the nuclei of endothelial cells lining the vessel lumen (L), valve (V), and valve sinus (S) of the human saphenous vein. Higher magnification images of the boxed regions are shown below. White dotted lines indicate luminal venous endothelial cells and green dotted lines indicate peri-valvular endothelial cells. The results shown are representative of 4 samples studied for each group.

Supplemental Figure 2.



Supplemental Figure 2. Human peri-valvular endothelial expression of FOXC2, PROX1, and thrombosis-related proteins. A, FOXC2 and PROX1 were measured in the human saphenous vein using anti-FOXC2 and anti-PROX1 antibodies. Staining at the venous lumen prior to the valve (L), the luminal face (VL) and the sinus face (VS) of the valve, and the sinus wall (S) are shown at higher magnification below. B-E, Human saphenous veins were immunostained to detect expression of vWF, THBD, EPCR and TFPI. Staining at venous lumen prior to the valve (L), the luminal face (VL) and the sinus face (VS) of the valve leaflet, and the sinus wall (S) are shown at higher magnification below. The images shown are representative of those obtained from studies of 4 different individuals.

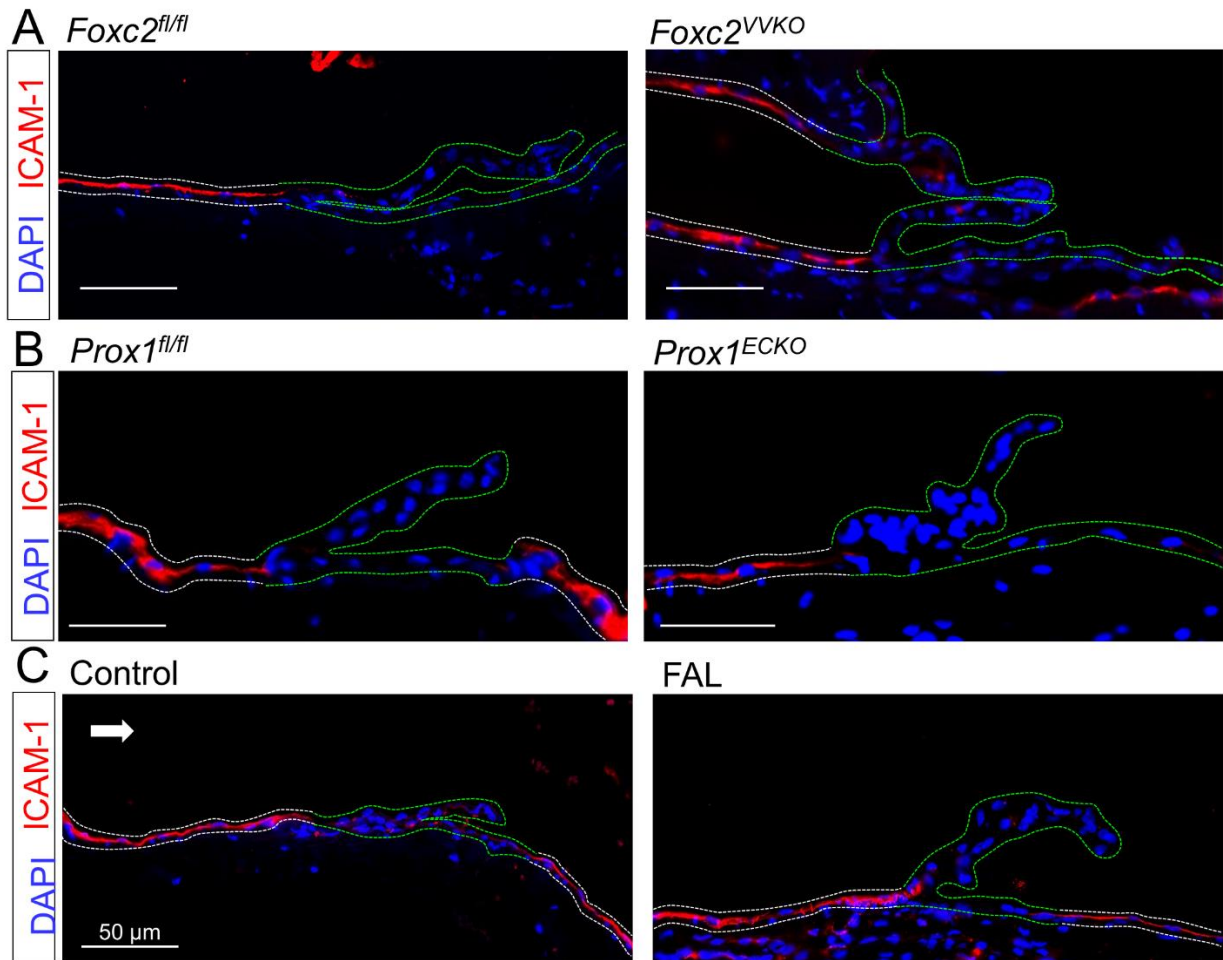
Supplemental Figure 3.



Supplemental Figure 3. Loss of PROX1 results in loss of TFPI without change in FOXC2,

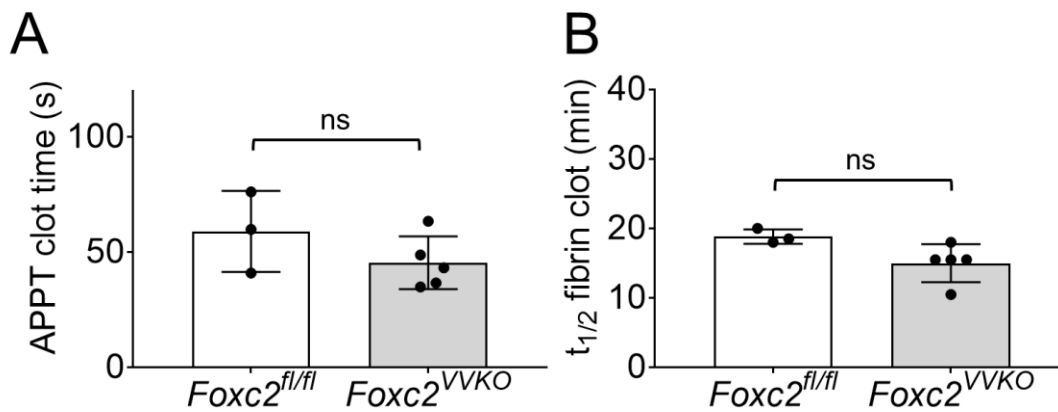
THBD, EPCR or vWF expression in peri-valvular venous endothelial cells. Immunostaining of mouse saphenous veins was performed in animals lacking PROX1 in endothelial cells (*Prox1^{ECKO}* mice) and littermate controls (*Prox1^{fl/fl}* mice). **A, B**, Loss of PROX1 does not alter peri-valvular endothelial expression of FOXC2. **C-E**, Loss of PROX1 does not change perivalvular endothelial expression of the anti-thrombotic proteins THBD and EPCR or the prothrombotic protein vWF. **F**, Loss of PROX1 results in loss of expression of the anti-thrombotic protein TFPI. White dotted lines indicate luminal venous endothelial cells and green dotted lines indicate peri-valvular endothelial cells. For all graphs the mean is represented by the bar and each dot represents a replicate, and error bars indicate standard deviation. Significance between the lumen endothelium for each condition and the sinus endothelium for each condition was determined by paired two-tailed Mann-Whitney test. ns indicates no significant difference; * indicates $p < 0.05$; ** indicates $p < 0.01$; *** indicates $p < 0.005$; **** indicates $p < 0.0001$.

Supplemental Figure 4.



Supplemental Figure 4. ICAM1 expression is not changed by FAL or genetic loss of FOXC2 or PROX1. A-C, Representative images of immunostaining for ICAM1 (red) expression was performed using the saphenous venous valves of *Foxc2^{fl/fl}* (n = 4) and *Foxc2^{VVKO}* (n = 4) mice (A), and *Prox1^{fl/fl}* (n = 6) and *Prox1^{ECKO}* (n = 4) mice(B), and mice subjected to 72 hours of FAL (n = 5) or control mice (n = 8) (C).

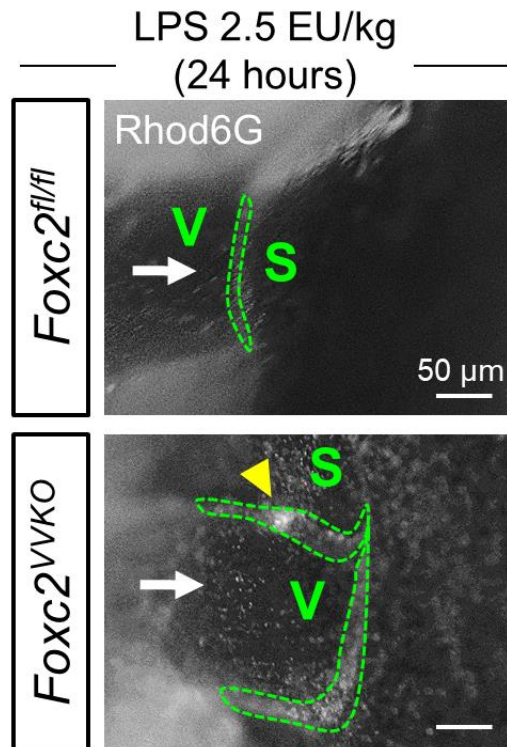
Supplemental Figure 5.



Supplemental Figure 5. *Foxc2^{VVKO}* mice have normal blood coagulability.

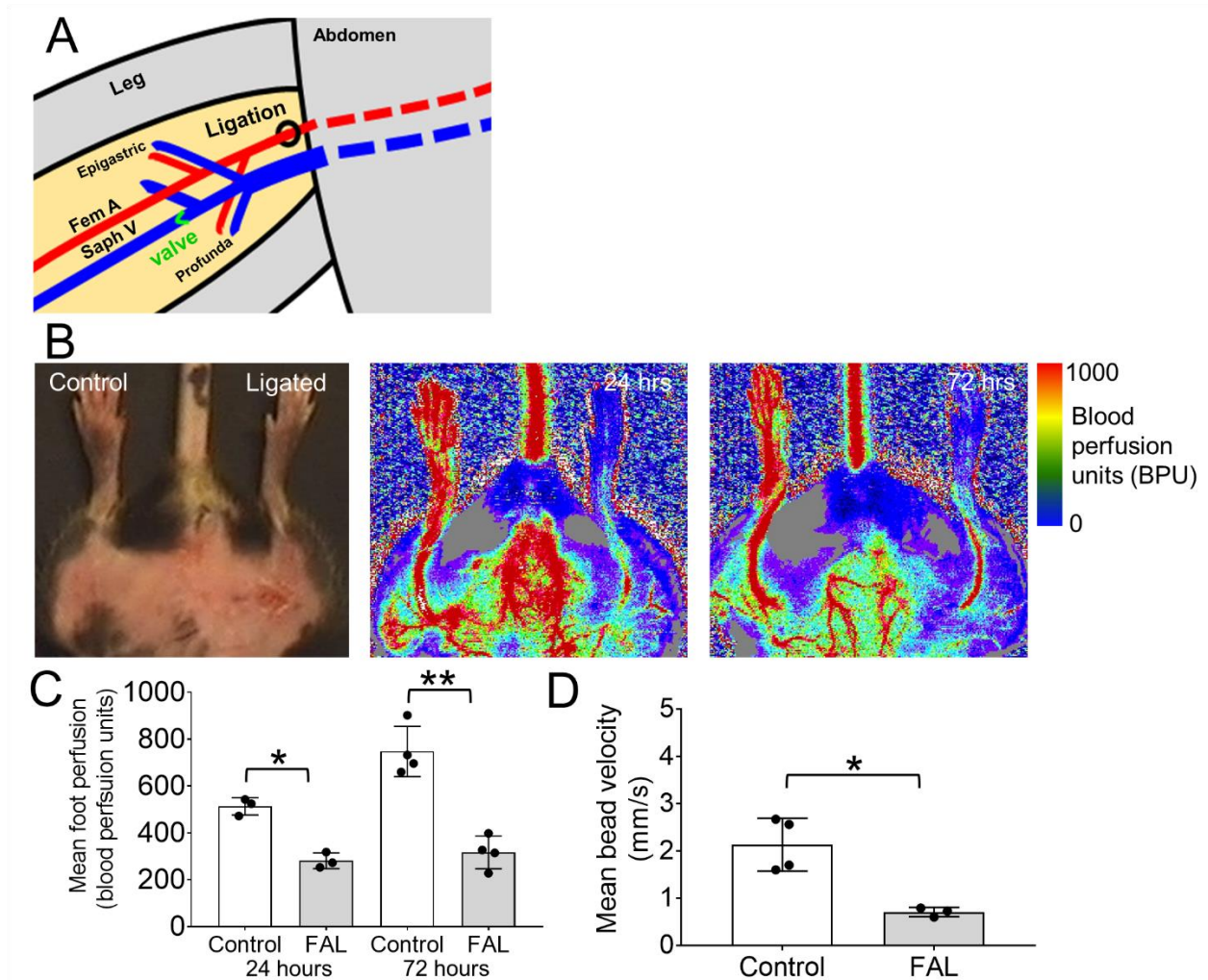
A, Quantification of mean activated partial thromboplastin time (APPT) for both *Foxc2^{fl/fl}* (white bars, n = 3 mice) and littermate *Foxc2^{VVKO}* mice (grey bars, n = 5 mice) is shown. **B**, Quantification of the half-time of well-plate fibrin clot formation for both *Foxc2^{fl/fl}* (white bars, n = 3 mice) and littermate *Foxc2^{VVKO}* mice (grey bars, n = 5 mice) is shown. For both graphs the mean is represented by the bar and each dot is a replicate, and error bars indicate standard deviation. Significance was determined by unpaired, two-tailed t-test. ns indicates no significant difference.

Supplemental Figure 6



Supplemental Figure 6. LPS stimulation induces spontaneous thrombosis in the sinus of deep venous valves of *Foxc2^{VVKO}* mice. Representative images of venous valves at the junction of the inferior vena cava and a lumbar vein in either *Foxc2^{fl/fl}* (top) or *Foxc2^{VVKO}* (bottom) mice 24 hours after intraperitoneal injection of 2.5 EU/kg LPS are shown. Leukocytes and platelets were visualized by infusion of Rhodamine 6G prior to intravital imaging. Blood flow direction is shown in each image with a white arrow and a stable thrombus identified in the *Foxc2^{VVKO}* animal is shown with the yellow arrowhead. These images are representative of 8 control mice and 12 knockout mice, quantitative data is in Supplemental Table 1.

Supplemental Figure 7

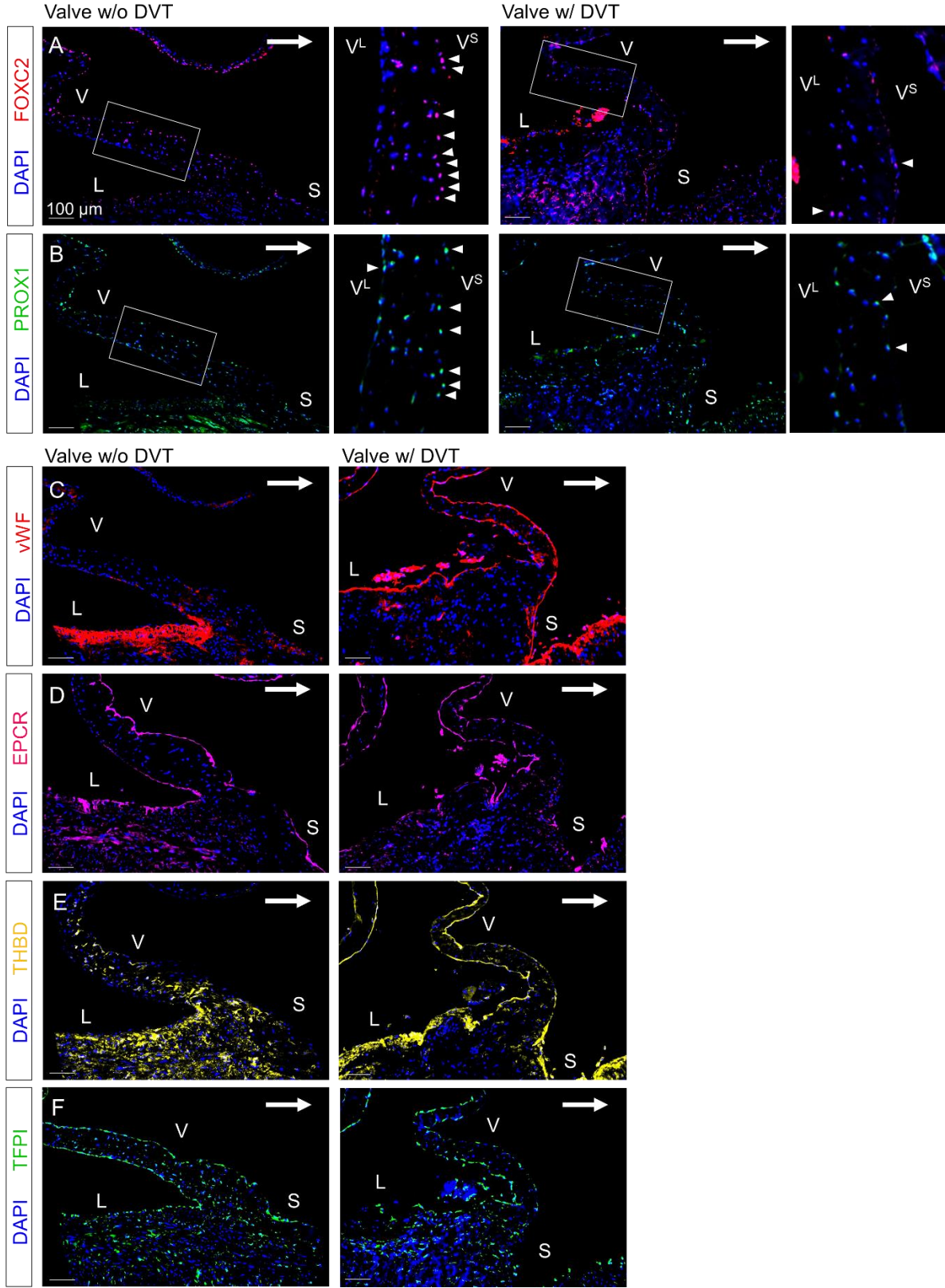


Supplemental Figure 7. Hemodynamic changes following femoral artery ligation in mice.

A, Schematic depiction of the site of femoral artery ligation proximal to the femoral artery bifurcation, and distant from the saphenous vein valve (green). **B**, Laser Doppler imaging of total leg blood flow 24 and 72 hours after femoral artery ligation. **C**, Quantification of mean blood perfusion of the control foot (white bars) and the foot on the side of the femoral artery ligation (grey bars) 24 and 72 hours after ligation. Each time point is a distinct experiment with different groups of mice. **D**, Quantification of the mean velocity of infused fluorescent beads in the mouse saphenous vein in the control leg (white bar) and the leg with the femoral artery ligation (grey

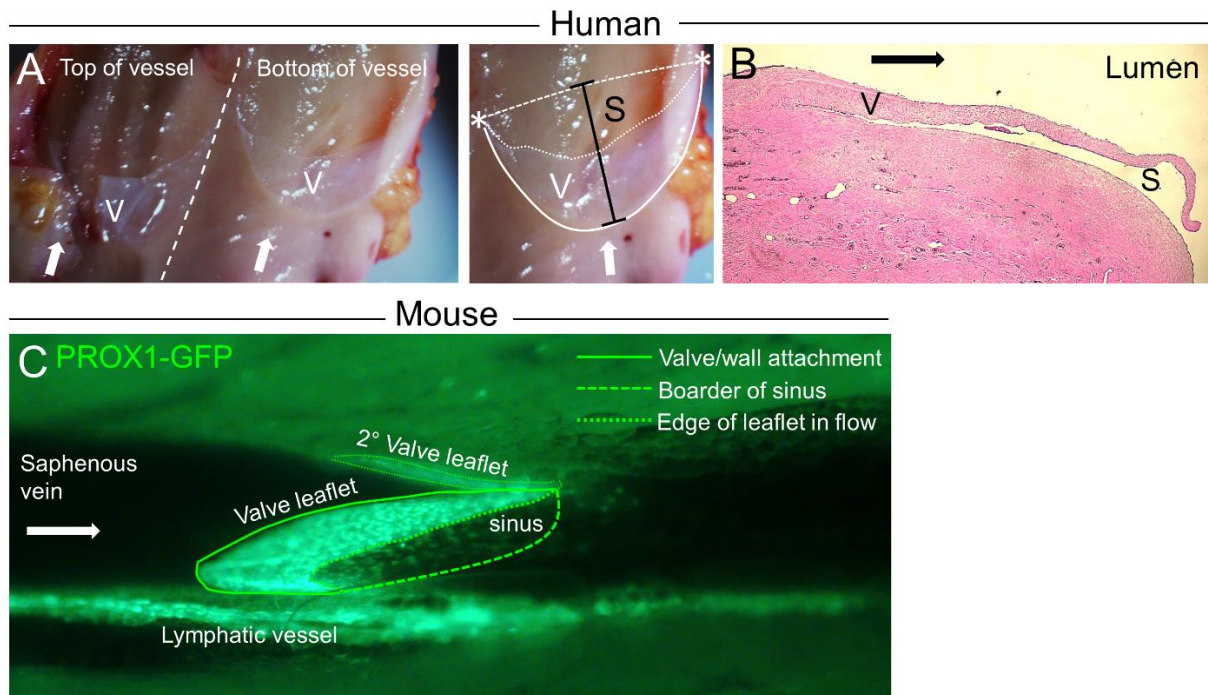
bar) 72 hours after femoral artery ligation. Dots represent individual mice measurements and error bars indicate standard deviation. Significance was determined by unpaired, two-tailed t-test. ns indicates no significant difference; * indicates $p < 0.05$; ** indicates $p < 0.01$.

Supplemental Figure 8



Supplemental Figure 8. Human DVT arises in association with loss of the peri-valvular endothelial transcription factor and anti-thrombotic phenotypes. Immunostaining for **A**, FOXC2 and **B**, PROX1 were performed on valves with and without DVT harvested from a second individual following death due to massive pulmonary embolism. Regions of the endothelium are shown as vessel wall in the lumen (L), along the valve (V), and vessel wall in the valve sinus (S). Insets show zoom in of the boxed area. V_L indicates the luminal face of the valve and V_s is the sinus face of the valve. Arrowheads indicate “positive” nuclei. **C-D**, immunostaining for vWF, EPCR, THBD and TFPI on adjacent sections of valves with and without DVT are shown. Arrows indicate the direction of blood flow.

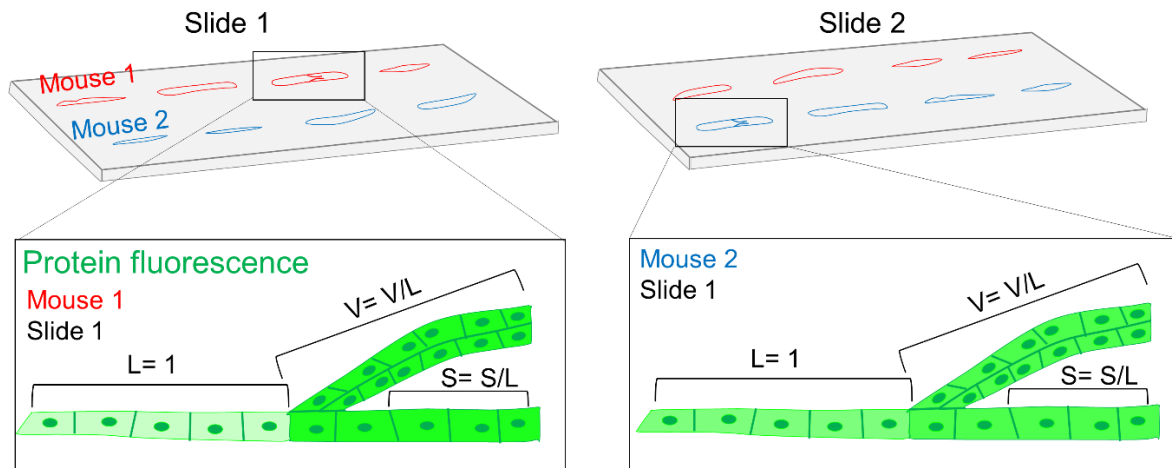
Supplemental Figure 9



Extended data Figure 9. Identification of the valve and valve sinus in human and mouse

veins. **A**, Image of a human venous valve leaflet (V) after longitudinal section of the vessel. The valve leaflets connect to the vessel wall across half of the vessel, and terminate in a downstream left and right vertex points (white stars). The valve sinus region is defined as the wall endothelium behind the valve leaflets extending to the vertex points on both sides (S, black line). **B**, Cross-sectional H-E staining of a human saphenous venous valve (V) and sinus (S) region. **C**, Intravital image of a saphenous venous valve leaflet and sinus (green outlines) in a Prox1-GFP transgenic mouse.

Supplemental Figure 10



Extended data Figure 10. Venous valve immunostaining and quantification. Due to the very small tissue size of the mouse saphenous vein it is technically difficult to get slides that consistently contain sections with venous valves present in the sample. This is represented in the schematic showing Slide 1 (left) and Slide 2 (right) with sections from Mouse 1 (red) and Mouse 2 (blue). Slide 1 contains a section with the venous valve visible from Mouse 1 but not Mouse 2. Conversely, Slide 2 has a section with the valve from Mouse 2 visible. The enhanced images show a schematic of how the lumen (L), valve (V), and sinus (S) endothelium are defined. To account for slide-to-slide differences in staining each sample is internally controlled to the lumen (L) signal intensity. V and S values are then reported as fold-increase to their respective lumen.

Supplemental Table 1.

Genotype	LPS (EU/kg)	Spontaneous micro-thrombi	P value
<i>Foxc2^{fl/fl}</i>	0	0 / 14	--
<i>FoxC2^{VVKO}</i>	0	6 / 17	0.005
<hr/>			
<i>Foxc2^{fl/fl}</i>	2.5	1 / 8	--
<i>FoxC2^{VVKO}</i>	2.5	8 / 12	0.0281

Supplemental Table 1. Quantification of spontaneous thrombus formation.

Supplemental Movie Legends

Supplemental Movie 1. Mouse saphenous vein blood flow after femoral artery ligation.

Mouse saphenous blood flow was observed by tracking fluorescent microparticles (red) after retro-orbital injection. The first video shows bead flow in the leg without femoral artery ligation (flow left to right). The second video shows bead flow in the leg with femoral artery ligation (flow right to left).

Supplemental Movie 2. Human venous valve ultrasound. Popliteal venous flow around the site of a venous valve was measured using 2D color Doppler in a healthy volunteer. Forward flow (right to left) is shown in blue, and reversing flow in red. The first part of the movie shows venous flow under immobile conditions and the second part during an active toe curl.

Supplemental Movie 3. Human venous valve ultrasound with ICD. Saphenous venous flow around the site of a venous valve was measured using 2D color Doppler in a healthy volunteer. Forward flow (right to left) is shown in blue, and reversing flow in red. The first part of the movie shows venous flow during an active toe curl, and the second part of the video shows venous flow during ICD compression.